A hybrid Hilbert Huang transform and improved fuzzy decision tree classifier for assessment of power quality disturbances in a grid connected distributed generation system

Ranjeeta Bisoi*, Tatiana Chakravorti and Nihar Ranjan Nayak

Siksha 'O' Anusandhan (Deemed to be University),
Multidisciplinary Research Cell,
University Campus,
Khandagiri Square, Bhubaneswar – 751030, Odisha, India
Email: ranjeeta.bisoi@gmail.com
Email: tatiana.chakravorti@gmail.com
Email: nihar.microsys@gmail.com
*Corresponding author

Abstract: This paper focuses on discrete Hilbert Huang transform (HHT) and improved fuzzy decision tree (IFDT)-based detection and classification of power quality (PQ) disturbances as a new contribution to the literature. A distributed generation (DG)-based microgrid has been modelled with wind and solar. Different PQ disturbances have been simulated with various wind speed and PV penetration. The PQ signals are passed through empirical mode decomposition (EMD) to obtain the intrinsic mode functions (IMFs). These IMFs are enforced to the Hilbert transform (HT) to extract the instantaneous attributes. These attributes of Hilbert transform (HT) are used for features extraction. Based on these extracted features improved fuzzy rules are formed for classification of the PQ disturbances. Synthetically PQ disturbances are simulated to check the performance of the proposed method. All these signal samples are processed through the proposed algorithm. The proposed method has been found to be capable of accurate detection and classification of PQ disturbances than many other techniques in the literature.

Keywords: distributed generations; DG; Hilbert Huang transform; HHT; improved fuzzy decision tree; IFDT; pattern recognition; power quality disturbances.

Reference to this paper should be made as follows: Bisoi, R., Chakravorti, T. and Nayak, N.R. (2020) 'A hybrid Hilbert Huang transform and improved fuzzy decision tree classifier for assessment of power quality disturbances in a grid connected distributed generation system', *Int. J. Power and Energy Conversion*, Vol. 11, No. 1, pp.60–81.

Biographical notes: Ranjeeta Bisoi is currently working as a Research Officer in the Multidisciplinary Research Cell of the Siksha 'O' Anusandhan (Deemed to be University), Bhubaneswar, India. She received her Master in Computer Application in 2011 from the North Orissa University, Orissa, India and PhD in Computer Science Engineering in 2015 from the Siksha 'O' Anusandhan (Deemed to be University), India. She has published 25 papers in International journals and conferences. Her research interests include soft computing, data mining, machine intelligence, bioinformatics, and classification.

Tatiana Chakravorti is working as a Research Associate at Siksha O Anusandhan (Deemed to be University), Bhubaneswar, Odisha, India. She has completed her Mtech. in Electronics and Communication Engg., from the Netaji Subhash Engineering College under West Bengal University of Technology in 2014 and completed her Btech from the Dream Institute of Technology under West Bengal University of technology in 2011. Her research interests include pattern recognition and classification, renewable energy, adaptive filtering, intelligent system.

Nihar Ranjan Nayak received his BEng in Electronics and Telecommunication in 1992 from the Utkal University, Bhubaneswar, India and MTech in Communication System Engineering in 2004 from the Biju Patnaik University of Technology, Bhubaneswar, India. Currently he is working for PhD at Siksha 'O' Anusandhan (Deemed to be University), Bhubaneswar, India. His research interests include signal processing, pattern recognition, classification.

1 Introduction

Generation, transmission, and distribution are the three functional blocks of an electrical system. The generation of power should be sufficient and the quality should be good; so that the customers' demand can be fulfilled and the devices have a long life. But due to the use of power electronic devices (PEDs) and sensitive loads, the required amount of power cannot be delivered as it introduces the power line disturbances in the system. The uses of these PEDs increase the accessibility to power quality (PQ) disturbances in the system. These disturbances cause deviation in voltage or frequency from its nominal value and eventually the quality of power decreases. The distribution side is more prone to the PQ disturbances. The PQ disturbances involve voltage sag, swell, notch, transient, harmonics and the multiclass PQ disturbances such as sag with harmonics and swell with harmonics etc. There are various PQ monitoring techniques have been proposed in the literature.

The most known technique is the Fourier transform (FT), which reckons on the data that are strictly linear or stationary with respect to time. Santoso et al. (2000) presents FT that categorise the steady state aspect of PQ disturbances but unable to categorise the transients. To overcome this shortcoming of FT, short-time Fourier transform (STFT) has been introduced, it divides the signal into two dimensional functions of frequency and time but it uses a stationary window which gives a fixed frequency range and gives good result in perception of harmonic (Gu and Bollen, 2000). Chen et al. (2007) proposes wavelet transform (WT) where they have analysed the various PQ disturbances in both time and frequency domain and it is more sensitive to distorted signals. WT implements on certain range of frequency so the magnitude calculation is not possible for all frequencies and under noisy condition the performance degrades. As the accuracy of performance depends on the choice of window and the level of decomposition of the signals so these are very important. Jurado and Saenz (2002) analysed two signal processing methods, those are STFT and WT on a 13 bus system. Chandel et al. (2008) presents the PQ disturbances classification using WT and artificial neural network (ANN). Abdullah et al. (2007) consider two methods based on time-frequency analysis

i.e., Gabor transform and spectrogram to analyse the PQ disturbances. Lee and Dash (2003) describe S Transform (ST) as phase corrected continuous WT, it implement multi-resolution on time differing signal as the window is movable and expandable. The width of the window is inversely proportional to the frequency which gives a high frequency resolution at low frequency and high time resolution at high frequency. The application of ST with neural network and extreme learning machine is suggested in Kaewarsa (2009), Bhende et al. (2008), Mishra et al. (2008) and Eristi et al. (2014) for classification of various PQ disturbances. Biswal and Dash (2013) presents a combination of fast variant ST and fuzzy decision tree (FDT) for the identification and classification of twelve PQ disturbances combine with noise and without noise. Dash et al. (2003) uses S-transform to detect the high frequency burst of PQ disturbances. This method gives very good frequency resolution on signals of long period. Kaewarsa (2009) proposes a method to classify PQ disturbances using S-transform and ANN. The normalised features are given as input to the feed-forward neural network that is trained by back propagation method. The method requires less features and memory space and can classify the disturbances with a very high accuracy even in presence of noise. Janik and Lobos (2006) presents PQ events classification using support vector machine and radial basis function networks. It uses three-phase signal space phasor for extraction of features. All these techniques (Abdel-Galil et al., 2004; Kezunovic and Rikalo, 1996; Huang et al., 2002; Tong et al., 2006 Biswal et al., 2014; Hu et al., 2005; Pei and Yeh, 2000; Li et al., 2000; Lee et al., 1994; Espinosa et al., 2010; Chang et al., 2011) have its own strengths and weaknesses.

In the last few years there are many advance techniques have been proposed by the researchers for PQ disturbance detection and classification, but the application of HHT with improved fuzzy has not been considered in a microgrid scenario. In this paper a combination of Hilbert Huang transform (HHT) and improved fuzzy decision tree (IFDT) is proposed for the detection and classification of PQ disturbances as a new contribution to the literature. A vast study has been done with this combined method to show its vast capability of monitoring. The performance of this method has been compared with other established methods and it has been found that the proposed combined method is capable of accurate detection than many other established techniques.

2 Hilbert Huang transform

For non-stationary signals, the amplitude and frequency changes with respect to time. To represent the exact sinusoid form we require the values at each instant. To get the instantaneous values a signal is divided into mono component. To extract the mono component of the signal empirical mode decomposition (EMD) is applied. EMD decomposes a signal into multiple single components called intrinsic mode functions (IMFs). To retrieve the instantaneous parameters Hilbert transform (HT) is applied to the output of EMD. These instantaneous parameters are used to extract the features.

2.1 Empirical mode decomposition

EMD decomposes a non-periodic and non-stationary signal into single and symmetric component called IMFs. IMFs are consists of single frequency component and are arranged from highest to lowest frequency. The IMFs are retrieved from the signal using the sifting process. Huang et al., describes a function to be an IMF if it fulfil two conditions

1 The number of zero crossing and the number of extreme of a data set must be equal or differ by at most one.

2 The mean of local maxima and local minima is zero at any point.

The algorithm for sifting process of a signal $X(t)$

Step1 Cubic spline interpolation is applied to the local maxima and local minima to get the maxima envelope, $M(t)$ and the minima envelope, $m(t)$, i.e., by linking all the respective local maxima and local minima.

Step 2 The average of the maxima envelope and minima envelope is calculated

$$E_1(t) = (M(t) - m(t))/2 \tag{1}$$

Step 3 Deduct the average of the envelope from the original signal to achieve the first IMF, i.e., IMF1

$$F_1(t) = X(t) - mE_1(t) \tag{2}$$

Step 4 $F_1(t)$ is the first IMF, if it fulfilled the given condition. If not then steps 1–3 is repeated assuming $F_1(t)$ as the signal data for next sifting process.

$$F_2(t) = F_1(t) - E_2(t) \tag{3}$$

where $E_2(t)$ is the average of envelopes of $F_1(t)$

Step 5 Determine the residue signal, $U_1(t)$

$$U_1(t) = X(t) - F_1(t) \tag{4}$$

Step 6 The procedure is repeated from step 1–5 to obtain the next IMFs. Terminate the EMD process when the value is above the threshold and reflects a mono tone signal data.

The sifting process can be wind up by choosing a value between the thresholds

$$SD = \sum_{t=0}^{T} \frac{\left|F_{n-1}(t) - F_n(t)\right|^2}{\left|F_n(t)\right|^2} \tag{5}$$

where $F_{n-1}(t)$, $F_n(t)$ are two successive sifting process.

2.2 Hilbert transform

The IMFs obtained from the EMD process are transformed by HT to obtain instantaneous amplitude (IA), instantaneous phase (IP), instantaneous frequency (IF). The HT converts the original signal into an analytic signal which contains the original signal as the real part and the 90º phase shifted signal of the original signal as the imaginary part. The IA, IP, IF depends upon the respective amplitude, phase, frequency of the original signal.

HT of a signal $R(t)$ can be expressed as:

$$\hat{R}(t) = \frac{1}{\pi} I \int_{-\infty}^{\infty} \frac{R(k)}{t-k} dt \tag{6}$$

where I = Cauchy integral principle

The transformed signal can be written as:

$$H(t) = R(t) + j\hat{R}(t) \tag{7}$$

a Instantaneous amplitude

$$IA = \sqrt{R^2(t) + \hat{R}^2(t)} \tag{8}$$

b Instantaneous phase

$$IP = \tan^{-1}\left[\frac{\hat{R}(t)}{R(t)}\right] \tag{9}$$

c Instantaneous frequency

$$IF = \frac{1}{2\pi}\frac{d}{dt}\tan^{-1}\left[\frac{\hat{R}(t)}{R(t)}\right] = \frac{1}{2\pi}\frac{R(t)\dot{\hat{R}}(t) - \hat{R}(t)\dot{R}(t)}{\left[R(t)^2 - \hat{R}(t)^2\right]} \tag{10}$$

To speed up the computational process of the continuous HT a discrete version (Pei and Yeh, 2000) is adopted here. The transfer function of the discrete HT is given by

$$H(\omega) = \begin{cases} j, \ldots\ldots, 0 < \omega < \pi \\ 0, \ldots\ldots, \omega = 0 \text{ and } \omega = \pi \\ -j, \ldots\ldots, -\pi < \omega < 0 \end{cases} \tag{11}$$

Consider an array of signal samples $x(k)$, $k = 1, 2, \ldots\ldots N$ for computing its DFT as

$$X = DFT(x(k), k = 1:N) \tag{12}$$

and its elements are obtained as $X(n) = \sum_{i=1}^{N} x(k) e^{(-2\pi j(n-1)(k-1))}$, $j = \sqrt{-1}$

A mask function M is defined as

$M = \{0, j, j, \ldots\ldots\ldots\ldots, 0, -j, -j, \ldots\ldots\ldots\ldots, -j\}$ if n is even

$M = \{0, -j, -j, \ldots\ldots\ldots\ldots, 0, j, j, \ldots\ldots\ldots\ldots, j\}$ if n is odd

The inverse *DFT* of the convoluted X is computed as

$$H(k) = R(k) + j\hat{R}(k) = IDFT[X * M] \tag{13}$$

Therefore using the discrete HT, the instantaneous amplitude and phase of the signal samples are obtained as

$$IA(k) = \sqrt{\left[R(k)^2 + \hat{R}(k)^2\right]},\ IP(k) = \tan^{-1}\left[\hat{R}(k)/R(k)\right] \tag{14}$$

2.3 Synthetic signals

To generate the PQ disturbance signals synthetically numeric modelling is used for simulation in MATLAB. These numeric models are formed as per the IEEE standards (Eristi et al., 2014). Multiple PQ disturbances such as sag with harmonics and swell with harmonics have been generated. The numeric model of single and multiple PQ disturbances are given in Table 1. PQ synthetic signals have been generated to test the HHT algorithm. Synthetically generated outputs of the proposed method of voltage sag and harmonics have been given in Figure 1 and Figure 2.

Table 1 Numeric modelling of PQ disturbances

PQ disturbance	*Numerical model*	*Parameters*
Pure sine	$X(t) = A \sin \omega t$	$A = 1(p.u)$, $\omega = 2\pi\ 50$ /radsec
Sag	$X(t) = (1 - \alpha(u(t - t_1) - u(t - t_2))) \sin \omega t$	$0.1 \le \alpha \le 0.9$, $T \le t_2 - t_1 \le 9T$
Swell	$X(t) = (1 + \alpha(u(t - t_1) - u(t - t_2))) \sin \omega t$	$0.1 \le \alpha \le 0.8$, $T \le t_2 - t_1 \le 9T$
Harmonics	$X(t) = \alpha_1 \sin(\omega t) + \alpha_3 \sin(3\omega t) + \alpha_5 \sin(5\omega t) + \alpha_7 \sin(7\omega t)$	$0.05 \le \alpha_1, \alpha_3, \alpha_5, \alpha_7 \le 0.15$, $\sum a_i^2 = 1$
Notch	$X(t) = \sin(\omega t) - sign(\sin(\omega t)) \times \left[\sum_{n=0}^{9} b \times \{u(t - (t_1 + 0.02n)) - u(t - (t_2 + 0.02n))\}\right]$	$0.1 \le b \le 0.9$, $0 \le t_1, t_2 \le 0.5T$ $0.01T \le t_2 - t_1 \le 0.05T$
Transient	$X(t) = \sin(\omega t) + ae^{-\frac{t-t_1}{\tau}} \sin \omega_n (t - t_1)\ \{u(t_2) - u(t_1)\}$	$0.1 \le \alpha \le 0.9$, $T \le t_2 - t_1 \le 3T$, 8 ms $\le \tau \le$ 40 ms, $300 \le f_n \le$ 900 Hz
Sag with harmonics	$X(t) = (1 - \alpha(u(t - t_1) - u(t - t_2)))\ \alpha_1 \sin(\omega t) + \alpha_3 \sin(3\omega t) + \alpha_5 \sin(5\omega t) + \alpha_7 \sin(7\omega t)$	$0.1 \le \alpha \le 0.9$, $T \le t_2 - t_1 \le 9T$ $0.05 \le \alpha_1, \alpha_3, \alpha_5, \alpha_7 \le 0.15$, $\sum a_i^2 = 1$
Swell with harmonics	$X(t) = (1 - \alpha(u(t - t_1) - u(t - t_2))) \sin \omega t$ $\alpha_1 \sin(\omega t) + \alpha_3 \sin(3\omega t) + \alpha_5 \sin(5\omega t) + \alpha_7 \sin(7\omega t)$	$0.1 \le \alpha \le 1.8$, $T \le t_2 - t_1 \le 9T$ $0.05 \le \alpha_1, \alpha_3, \alpha_5, \alpha_7 \le 0.15$, $\sum a_i^2 = 1$

Figure 1 Synthetically generated voltage swell, (a) EMD output (b) HT of IMF1 (c) HT of IMF2 (d) HT of IMF3 (see online version for colours)

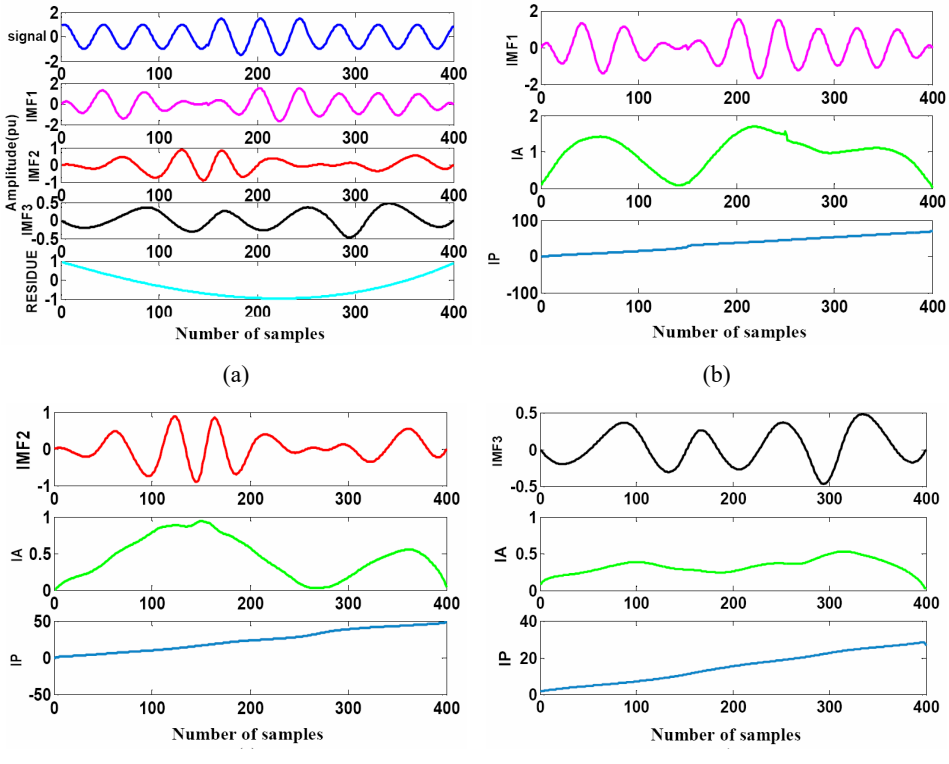

(a) (b)

(c) (d)

Figure 2 Synthetically generated harmonic, (a) EMD output (b) HT of IMF1 (c) HT of IMF2 (d) HT of IMF3 (see online version for colours)

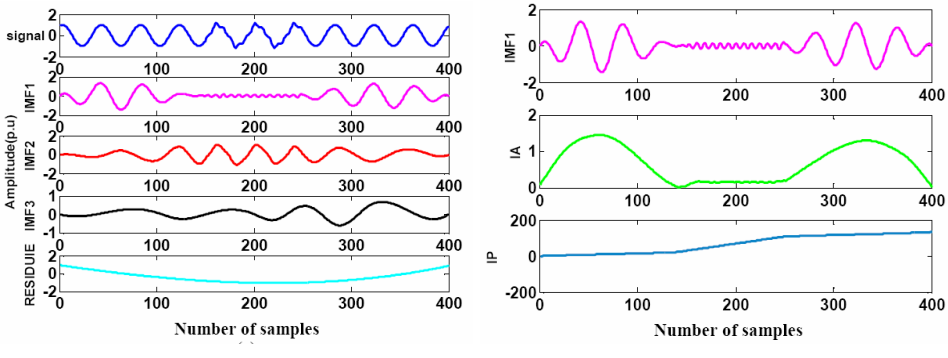

(a) (b)

Figure 2 Synthetically generated harmonic, (a) EMD output (b) HT of IMF1 (c) HT of IMF2 (d) HT of IMF3 (continued) (see online version for colours)

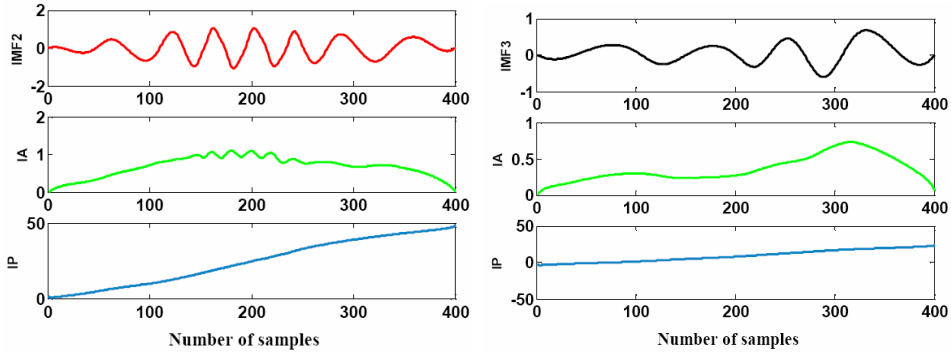

(c) (d)

3 Test system

In electrical systems, due to the use of solid state devices the deviation in magnitude, phase, and frequency occurs in the voltage and current waveforms. Rather than steady state disturbances, transients appear in the power system when back to back bank are switched. The operation of PEDs also produce harmonics, notches and sometimes some disturbances occurs simultaneously resulting in multiple disturbances like sag with harmonic and swell with harmonic. For the recognition of the disturbances data sets of PQ disturbances are required.

3.1 Signals generated by microgrid model

The one line diagram of the microgrid model, i.e., multiple DG-based microgrid model is illustrated in Figure 3. The model consists of two DGs, DG1 is the inverter-based photovoltaic solar farm and DG2 is the DFIG-based wind farm connected to 120 kV grid. The DGs are connected to the grid at the point of common coupling (PCC). To make the model more reliable a dc battery system is connected. The model is simulated with a sampling frequency of 3,840 Hz and nominal frequency of 60 Hz and the base voltage is 25 kV. The 25 kV PCC is connected to the utility grid with the help of transformer (Tr1). The grounding transformer (Tr2 and Tr3) are connected to the DGs. In order to simulate the PQ disturbances, the CBs are operated to insert the disturbances in the system. The order of opening and closing of CBs for disturbances class are as follows:

D1 voltage sag by closing CB8

D2 voltage swells by opening CB9

D3 harmonic by closing CB10

D4 voltage notching by opening CB11

D5 oscillatory transients by closing CB5

D6 unbalanced load switching by closing CB13

D7 voltage sag with harmonics by closing CB8 and CB10

D8 voltage swells with harmonic by opening CB9 and CB10.

Figure 3 DG-based microgrid model

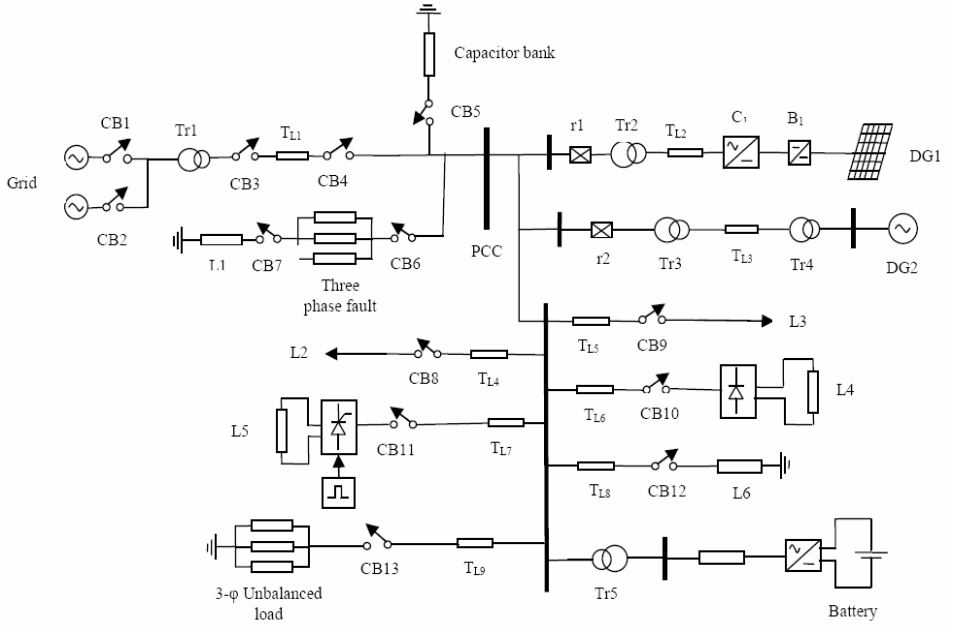

Table 2 PQ disturbance generated using microgrid model

PQ disturbances	*Events(D)*
Sag	D1
Swell	D2
Harmonic	D3
Notch	D4
Transient	D5
Unbalanced load	D6
Sag Harmonic	D7
Swell Harmonic	D8

The inverter-based PV solar farms uses 'Kyocera KD205GX-LP' PV module. Ten PV modules are connected in parallel to produce a 1 MW solar farm. Each module is consists of eight series connected modules per string and 61 parallel strings. The number of cells per string is 54. To extract the maximum power point perturb and observe method is used in this model. This method compares two consecutive instants power values that may increase or decrease the value to obtain the maximum power point.

Figure 4 Microgrid model generated voltage Sag, (a) EMD output (b) HT of IMF1 (c) HT of IMF2 (d) HT of IMF3 (see online version for colours)

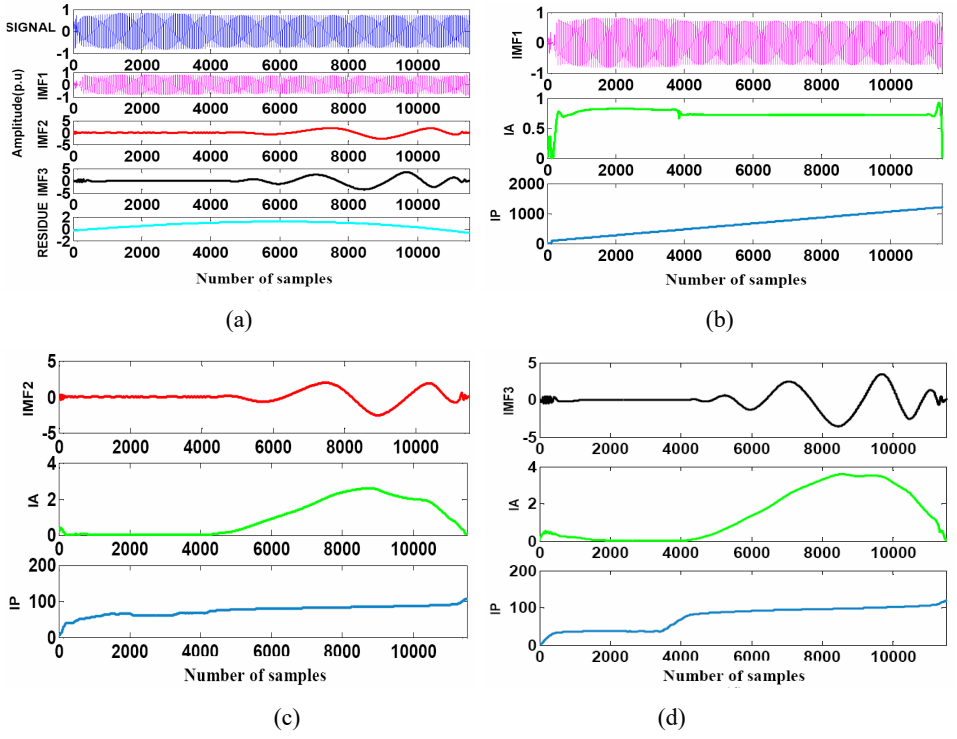

Table 3 Components and their specification of the Test System

Components	*Specification*
Utility grid	Rated kV = 120, f = 60 Hz, base voltage = 25 kV
Transformer(Tr1)	Rated MVA = 47,f = 60 Hz, rated kV = 120/25 R_1 and R_2 = 0.0015 pu, L_1 and L_2 = 0.03 pu, R_m = 200 pu, L_m = 200 pu
Transformer(Tr2,Tr3)	Rated MVA = 20,f = 60 Hz, rated kV = 25, R_o = 0.025 pu, X_o = 0.75 pu R_m = 500 pu, X_m = 500 pu
DG1 (photovoltaic-based solar farm)	Rated MW = 1, f = 60 Hz, V_{dc} = 500 V no. of cells in series = 8, no. of modules in parallel = 61
DG2 (DFIG-based wind farm)	Rated MW = 1.5, f = 60, rated voltage = 575 V, R_s = 0.023 pu, L_{1s} = 0.18 pu $R_{r'}$ = 0.016 pu, $L_{1r'}$ = 0.16 pu L_m = 2.9 pu, no. of wind turbines = 6
Transformer (Tr4)	Rated MW = 1.75, f = 60 Hz, rated voltage = 25 kV/ 575 V, R_1 and R_2 = 0.025/30 pu, L_1 and L_2 = 0.025 pu
Distribution lines (T_{L1}, T_{L2}, T_{L3}, T_{L4}, T_{L5}, T_{L6}, T_{L7}, T_{L8}, T_{L9})	Π-section, 10 Km each, r1 = 0.1153 Ω/Km, r0 = 0.413 Ω/Km l1 = 1.05 mH/Km, l0 = 3.32 mH/Km, c1 = 1.133 × 10^{-10} F/Km, c0 = 0.501 × 10^{10} F/Km.
Loads	Total load is 58 + j39MVar
Capacitor	Q_c = 50 MVar

A 9 MW DFIG-based wind farm consists of six 1.5 MW wind turbines connected in parallel. The wind turbine embodying DFIG which has a wound rotor induction generator and an insulated gate bipolar transistor (IGBT)-based PWM converter. The stator is directly connected to the utility grid and the rotor is fed at variable frequency through the voltage source converter. The wind speed is varied from 8 m/s to 20 m/s. The DFIG wind turbine is connected to the grid using a transformer (Tr4). All the events generated using the model and the model specification has been given in Table 2 and Table 3. The model output of voltage sag and sag with harmonics has been shown in Figure 4 and Figure 5.

Figure 5 Microgrid model generated sag with harmonic, (a) EMD output (b) HT of IMF1 (c) HT of IMF2 (d) HT of IMF3 (see online version for colours)

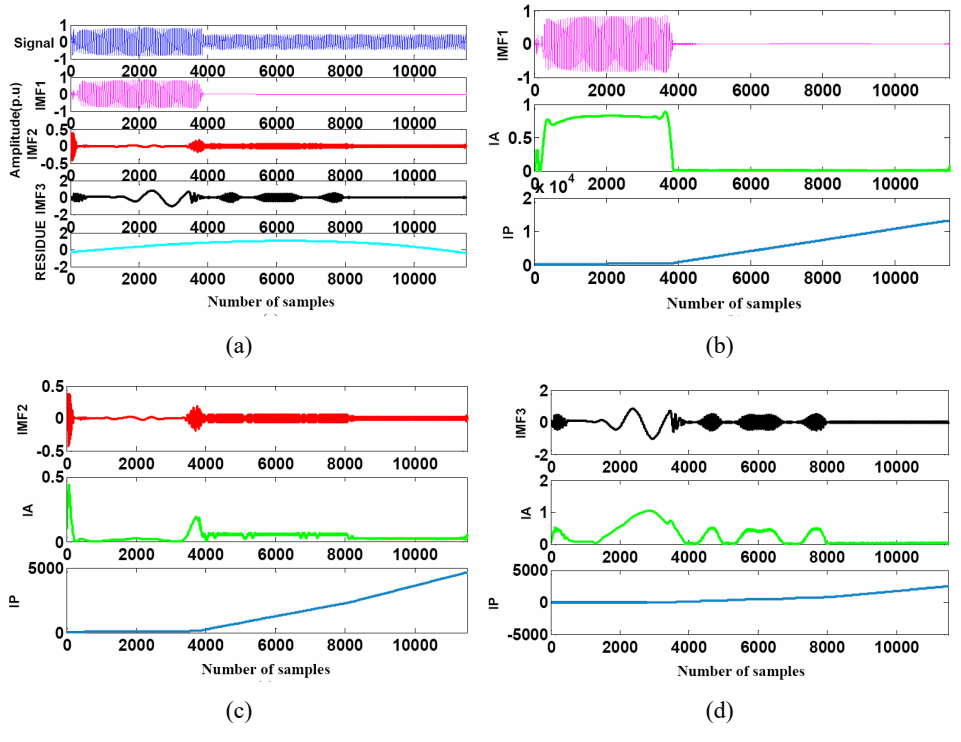

4 Target feature extraction

Features provide information to detect the PQ disturbances in a system as it resemblance the property of the original signal data. Higher IMF contains more frequency information than lower IMF. In different papers, authors have taken different number of IMFs as per their requirement. There are many classification papers in literature from which the idea has been taken. In this case, the features of first three IMFs are enough for the classification of PQ disturbances. In this paper all the features are extracted using the instantaneous parameters. Here we have considered entropy of IA (v_1), energy of IA (v_2), standard deviation of IA (v_3), standard deviation IP (v_4), maximum of IA (v_5) for pattern

identification. Separation of model generated PQ indices using entropy and standard deviation of IP of IMF1 are given in Figure 6.

- Entropy of IA

  It is defined as the measure of uncertainty of the data.

$$v_1 = \sum_{y=1}^{Y} \left(IA(y) \log_c IA(y) \right) \tag{15}$$

- Energy of IA

  It is defined as:

$$v_2 = \sum_{y=1}^{Y} IA(y)^2 \tag{16}$$

- Standard deviation of IA

  It is defined as the amount of dispersion in data set of IA.

$$v_3 = \sqrt{\frac{1}{Y-1} \sum_{y=1}^{Y} | IA(y) - \mu |^2} \tag{17}$$

  where, μ is the mean of the Y samples of IA

$$\mu = \frac{1}{Y} \sum_{y=1}^{Y} IA(y) \tag{18}$$

- Maximum of IA

  It is defined as the maximal value of IA.

Figure 6 Separation of PQ indices with entropy and standard deviation of IP of IMF1 (see online version for colours)

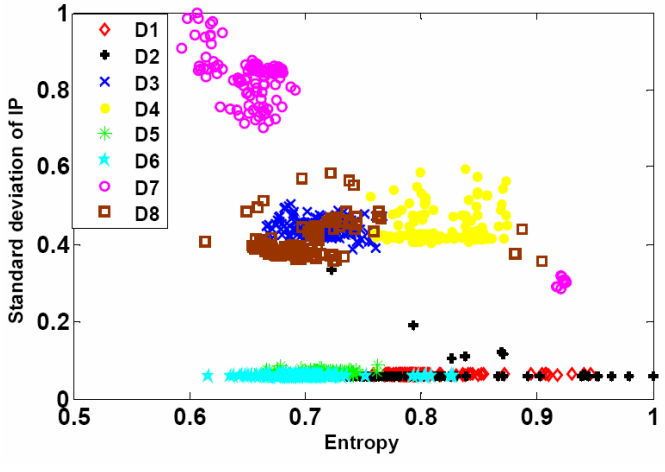

5 IFDT classifier

5.1 Improved fuzzy decision tree

For classification of multiple patterns and to distinguish between the overlapping values, an IFDT has been introduced. The computation for IFDT is simple and gives quite accurate results and it reduces the ambiguity in the pattern recognition. The traditional decision tree is different from IFDT as the splitting criteria in IFDT are depends on the certainty factor-based fuzzy conditions and the inference process is also different. The numeric training data is fuzzified to linguistic terms. A FDT is a directed acyclic graph in which each edge connects two nodes called as parent node and child node. Each node represents a fuzzy set. The node which has no parent node is called as root node and the node that has no child node is called as leaves. Till the stopping criterion is accomplished the parent node splits into two child node. The stopping criterion is selected such that the parent node can split into child node for definite number of observation. The splitting interval actuates the fuzzy boundaries that form the fuzzy rules for pattern recognition. By the application of Gini's diversity index and Towing's rule fuzzy rules are formulated. The split of correlated patterns are selected by Towing rule and the divergence between the target attribute values are measured by Gini's diversity index. For numerous patterns, let the number of patterns be q, the percentage of observation at the d^{th} node of i^{th} pattern is defined by W_{q1}, the Gini's diversity index is determined as:

$$GDI = \sum_{i=1}^{q} W_{qd}\left[1 - W_{qd}\right] \tag{19}$$

The complexity in computation and the accuracy for pattern recognition depends upon the size of the FDT. FDT is formed by the judgment rules that are formed by selecting the substantial value to attain the maximum accuracy. The fuzzy rules generate the membership function. The triangular membership functions are used to fuzzify the rules to form the FDT. The triangular membership function can be defined as, let the legs be b_1, b_2, b_3, and b be the input

$$\mu(b_1, b_2, b_3) = \left.\begin{array}{ll} 0 & \text{if } b < b_1 \\ \dfrac{b - b_1}{b_2 - b_1} & \text{if } b_1 \le b < b_2 \\ \dfrac{b_3 - b}{b_3 - b_2} & \text{if } b_2 \le b \le b_3 \\ 0 & \text{if } b_3 < b \end{array}\right\} \tag{20}$$

In this paper fuzzy rule-based classification has been improved using certainty factor which is considered as IFDT. In this paper, a, b and c are the membership points of triangular membership function of IMF 1. These three points represent the first, middle and last position of the triangular membership function of IMF 1, respectively. The certainty factor is build with support and confidence indices. The association rules are generated form $ANT_\tau \rightarrow CON_\tau$ where, '*ANT*' is the antecedents and '*CON*' is the consequents of the 'τ' assessment rules.

The support (S_τ) of a particular rule τ^{th} is mathematically defined as:

$$S_\tau\left(ANT_\tau - CON_\tau\right) = p\left(ANT_\tau \cap CON_\tau\right) = \frac{\sum_{N\in\zeta}\mu_{A_i}\left(X_N\right)}{\zeta} \tag{21}$$

where 'N' is the attributes (X) number and the number of membership function is defined as 'i', respectively. The confidence (C_τ) of a particular rule 'τ' is mathematically defined as:

$$C_\tau\left(ANT_\tau - CON_\tau\right) = \frac{p\left(ANT_\tau \cap CON_\tau\right)}{p\left(ANT\right)} = \frac{\sum_{N\in\zeta}\mu_{A_i}\left(X_N\right)}{\sum_{N=1}^{\zeta}\mu_{A_i}\left(X_N\right)} \tag{22}$$

The certainty factor (CF_τ) for a particular rule 'τ' is defined as:

$$CF_\tau = C_\tau\left(ANT_\tau \rightarrow CON_\tau\right) - \rho_\tau \tag{23}$$

The average confidence value ρ_τ for each rule is defined as:

$$\rho_\tau = \frac{1}{\zeta - 1}\sum_{\substack{N=1\\N\neq\zeta}}^{\zeta} C_\tau\left(ANT_\tau \rightarrow CON_n\right) \tag{24}$$

Table 4 Operating condition-based feature values of different PQ disturbances

DG	*Operating condition*	*Class*	V_1 *entropy of IA*	V_2 *energy of IA*	V_3 *std of IA*	V_4 *std of phase*	V_5 *maximum of IA*
DG1	8,100	D1	0.8524	0.6545	0.3477	0.1032	0.3754
DG1	20,100	D2	0.9459	0.7903	0.2121	0.0983	0.3037
DG1	81,000	D3	0.6667	0.0943	0.3406	0.6483	0.1036
DG1	201,000	D4	0.7565	0.1233	0.3009	0.6740	0.1260
DG1	8,100	D5	0.6537	0.8559	0.3129	0.1025	0.2323
DG1	20,100	D6	0.6168	0.8678	0.2553	0.0987	0.2204
DG1	81,000	D7	0.6256	0.1138	0.2768	0.6768	0.1132
DG1	201,000	D8	0.6136	0.1328	0.3248	0.5918	0.1002
DG2	20,100	D1	0.8127	0.7224	0.4273	0.1078	0.4128
DG2	81,000	D2	0.8945	0.8963	0.4956	0.3269	0.2789
DG2	201,000	D3	0.7668	0.1734	0.4107	0.7443	0.1294
DG2	8,100	D4	0.8741	0.1324	0.4262	0.8352	0.1472
DG2	20,100	D5	0.7083	0.9188	0.4010	0.1234	0.2499
DG2	81,000	D6	0.7220	0.9231	0.3031	0.0998	0.3123
DG2	201,000	D7	0.6925	0.1722	0.3648	0.8384	0.1289
DG2	8,100	D8	0.7588	0.1722	0.4641	0.7837	0.1445

Table 5 Membership points of triangular membership function of IMF1

Sl. no.	*IMF*	*Membership name*	*Class value*	*a*	*b*	*c*
1	IMF1	$\mu(v_1)A_1$	D7	0.5934	0.6593	0.7253
2	IMF1	$\mu(v_1)A_2$	D8	0.6136	0.6838	0.7540
3	IMF1	$\mu(v_1)A_3$	D5	0.6537	0.7083	0.7629
4	IMF1	$\mu(v_1)A_4$	D3	0.6667	0.7168	0.7668
5	IMF1	$\mu(v_1)A_5$	D6	0.6868	0.7570	0.8271
6	IMF1	$\mu(v_1)A_6$	D4	0.7865	0.8303	0.8741
8	IMF1	$\mu(v_1)A_7$	D1	0.8493	0.8976	0.9459
9	IMF1	$\mu(v_1)A_8$	D2	0.8609	0.9305	1.0000
10	IMF1	$\mu(v_2)B_1$	D8	0.0933	0.1328	0.1722
11	IMF1	$\mu(v_2)B_2$	D4	0.1044	0.1474	0.1903
12	IMF1	$\mu(v_2)B_3$	D3	0.1143	0.1639	0.2134
13	IMF1	$\mu(v_2)B_4$	D7	0.1256	0.2888	0.4519
14	IMF1	$\mu(v_2)B_5$	D1	0.6545	0.7224	0.7903
15	IMF1	$\mu(v_2)B_6$	D5	0.8559	0.9088	0.9616
16	IMF1	$\mu(v_2)B_7$	D6	0.8678	0.9231	0.9783
17	IMF1	$\mu(v_2)B_8$	D2	0.8831	0.9416	1.0000
18	IMF1	$\mu(v_3)C_1$	D6	0.2075	0.2553	0.3031
19	IMF1	$\mu(v_3)C_2$	D5	0.2906	0.3615	0.4323
20	IMF1	$\mu(v_3)C_3$	D4	0.3009	0.3786	0.4562
21	IMF1	$\mu(v_3)C_4$	D8	0.3248	0.3945	0.4641
22	IMF1	$\mu(v_3)C_5$	D3	0.3406	0.4107	0.4807
23	IMF1	$\mu(v_3)C_6$	D1	0.3477	0.4273	0.5069
24	IMF1	$\mu(v_3)C_7$	D2	0.3821	0.5806	0.7790
25	IMF1	$\mu(v_3)C_8$	D7	0.5792	0.7706	0.9621
26	IMF1	$\mu(v_4)D_1$	D6	0.0591	0.0868	0.1146
27	IMF1	$\mu(v_4)D_2$	D1	0.0718	0.1011	0.1303
28	IMF1	$\mu(v_4)D_3$	D5	0.0813	0.1139	0.1464
29	IMF1	$\mu(v_4)D_4$	D2	0.1589	0.2457	0.3325
30	IMF1	$\mu(v_4)D_5$	D3	0.3481	0.4256	0.5030
31	IMF1	$\mu(v_4)D_6$	D8	0.3543	0.4692	0.5841
32	IMF1	$\mu(v_4)D_7$	D4	0.4035	0.5000	0.5965
33	IMF1	$\mu(v_4)D_8$	D7	0.5556	0.7778	1.0000
34	IMF1	$\mu(v_5)E_1$	D3	0.1036	0.1294	0.1552
35	IMF1	$\mu(v_5)E_2$	D4	0.1247	0.1460	0.1672
36	IMF1	$\mu(v_5)E_3$	D8	0.1402	0.1645	0.1888
37	IMF1	$\mu(v_5)E_4$	D5	0.2056	0.2341	0.2625
38	IMF1	$\mu(v_5)E_5$	D6	0.2204	0.2874	0.3543
39	IMF1	$\mu(v_5)E_6$	D2	0.2387	0.3037	0.3687
40	IMF1	$\mu(v_5)E_7$	D1	0.3056	0.5254	0.7452
41	IMF1	$\mu(v_5)E_8$	D7	0.3353	0.5464	0.7576

Figure 7 Plot of membership functions of the extracted features of IMF1 of microgrid model signals, (a) entropy of IA (b) energy of IA (c) standard deviation of IA (d) standard deviation of IP (e) maximum value of IA (see online version for colours)

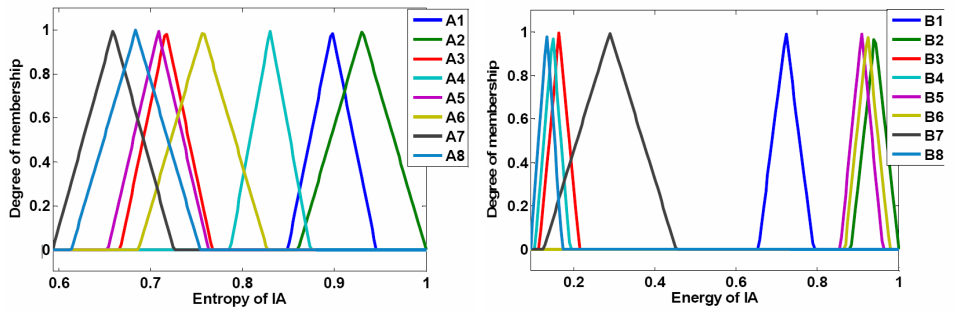

(a)

(b)

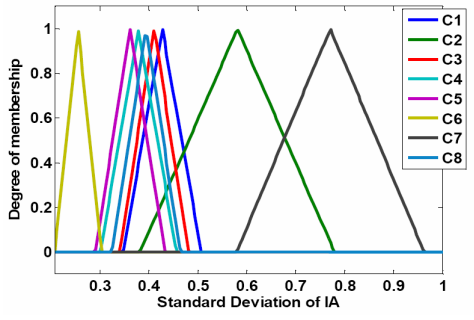

(c)

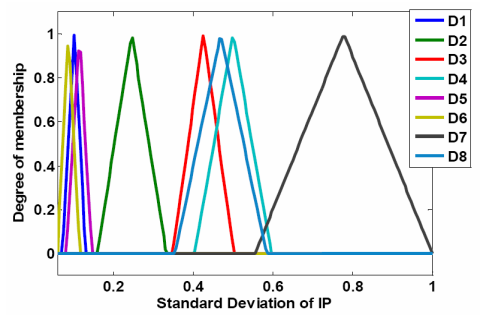

(d)

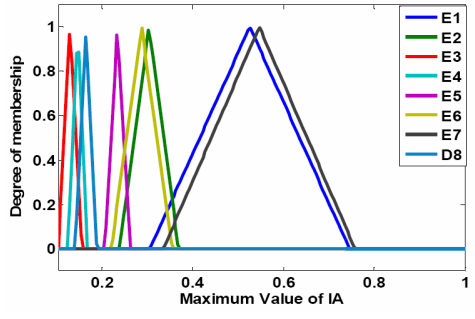

(e)

5.2 Improved fuzzy rule-base classification

The fuzzy rules are associated with the membership functions. In this paper first three IMFs are considered for the classification of PQ disturbances as per literature survey. For IFDT only IMF1 values are enough to classify the classes. That's why the IMF1 has been taken consideration in this paper. The membership points and the figures are given for only IMF1. In the microgrid scenario the authors have changed the wind speed and solar penetration and collected all the ranges for the disturbances. Table 4 shows the operating

condition-based feature values for PQ disturbances. Table 5 show the triangular membership points for IMF1and Figure 7 show the plot of the membership functions of IMF1.

Rule-base classification:

Rule 1 If v_1 is A_8 && v_2 is B_5 && v_3 is C_6 && v_4 is D_2 && v_5 is E_7. Then 'D1' with certainty factor CF_{R1}.

Rule 2 If v_1 is A_9 && v_2 is B_9 && v_3 is C_7 && v_4 is D_4 && v_5 is E_6. Then 'D2' with certainty factor CF_{R2}.

Rule 3 If v_1 is A_4 && v_2 is B_3 && v_3 is C_5 && z_4 is D_6 && v_5 is E_1. Then "D3" with certainty factor CF_{R3}.

Rule 4 If v_1 is A_6 && v_2 is B_2 && v_3 is C_3 && v_4 is D_8 && v_5 is E_2. Then 'D4' with certainty factor CF_{R4}.

Rule 5 If v_1 is A_3 && v_2 is B_7 && v_3 is C_2 && v_4 is D_3 && v_5 is E_4. Then 'D5' with certainty factor CF_{R5}.

Rule 6 If v_1 is A_5 && v_2 is B_8 && v_3 is C_1 && v_4 is D_1 && v_5 is E_5. Then 'D6' with certainty factor CF_{R6}.

Rule 7 If v_1 is A_1 && v_2 is B_4 && v_3 is C_8 && v_4 is D_8 && v_5 is E_8. Then 'D7' with certainty factor CF_{R7}.

Rule 8 If v_1 is A_2 && v_2 is B_1 && v_3 is C_4 && v_4 is D_7 && v_5 is E_3. Then 'D8' with certainty factor CF_{R8}.

6 Performance evaluation of the proposed classifier

The capability of the proposed method has been experimented with classification accuracy and sensitivity, so that we can demonstrate the capability of the proposed technique with other established methods. There are many papers in the literature from where it can be proved that both the techniques, Fuzzy and HHT, respectively, are real time feasible (Li et al., 2000; Lee et al., 1994; Espinosa et al., 2010; Chang et al., 2011). That's why the authors have chosen these techniques for classification problem. The generalisation capability of both the techniques is very high. Synthetic signals are generated using the mathematical modelling based on IEEE 1159 standards. The proposed method has been tested in different noisy conditions also. Accuracy for a particular pattern 'z' can be defined as:

$$AC_z(\%) = \frac{\begin{array}{c}\text{Tota l number of correctly classified patterns} \\ \text{for a particular event } 'z'\end{array}}{\text{Total number of patterns of a particular event } 'z'} \times 100 \tag{25}$$

The sensitivity (S_z) for a particular pattern 'z' can be defined as:

$$S_z(\%) = \frac{\text{NUmber of patterns for a particular event } 'x'}{\begin{array}{l}\text{Number of patterns of a particular event } 'x' \\ \quad + \text{Number of miscalssified patterns for a particular event } 'x'\end{array}} \times 100 \tag{26}$$

Table 6 Certainty factor values for Fuzzy rule base classification

Rules	*D1*	*D2*	*D3*	*D4*	*D5*	*D6*	*D7*	*D8*
CF_{R1}	0.964	0.012	0.009	0.005	0.004	0.002	0.002	0.002
CF_{R2}	0.014	0.961	0.008	0.004	0.006	0.002	0.003	0.002
CF_{R3}	0.009	0.012	0.956	0.011	0.004	0.003	0.003	0.002
CF_{R4}	0.005	0.009	0.015	0.939	0.017	0.007	0.004	0.004
CF_{R5}	0.001	0.001	0.002	0.011	0.974	0.009	0.001	0.001
CF_{R6}	0.010	0.009	0.005	0.005	0.016	0.933	0.015	0.007
CF_{R7}	0.010	0.005	0.012	0.005	0.009	0.009	0.941	0.009
CF_{R8}	0.012	0.009	0.014	0.012	0.009	0.014	0.018	0.912

Table 7 Confusion matrix for microgrid model generated PQ disturbances

Events	*D1*	*D2*	*D3*	*D4*	*D5*	*D6*	*D7*	*D8*
D1	297	2	0	0	0	0	1	0
D2	1	297	1	0	0	0	0	1
D3	0	0	297	0	1	0	2	0
D4	0	0	2	296	2	0	0	0
D5	0	0	0	1	299	0	0	0
D6	2	1	0	0	0	296	1	0
D7	1	0	2	0	1	0	295	1
D8	1	1	1	0	0	1	2	294

Figure 8 Classification accuracy of model generated different PQ events in different noisy conditions (see online version for colours)

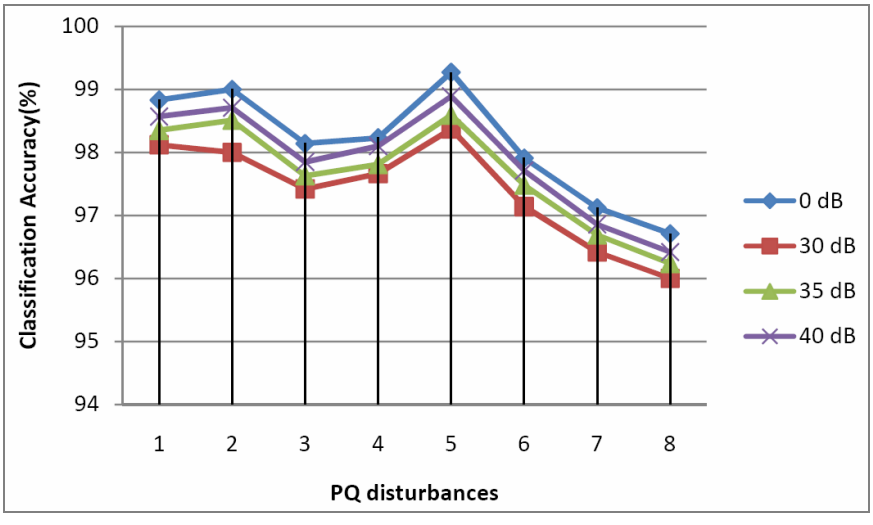

Table 8 Classification accuracy of the proposed method using Model generated signals in different noisy conditions

PQ disturbances	*Accuracy (%) (no noise)*	*Accuracy (%) (no noise)*	*Accuracy (%) (35db noise)*	*Accuracy (%) (40db noise)*
D1	98.83	98.12	98.35	98.57
D2	99	98	98.51	98.71
D3	98.14	97.42	97.63	97.85
D4	98.23	97.66	97.81	98.1
D5	99.27	98.37	98.59	98.89
D6	97.91	97.14	97.48	97.71
D7	97.12	96.42	96.69	96.86
D8	96.71	96	96.24	96.42
Average	98.15	97.39	97.66	97.88

Table 9 Sensitivity of the proposed method using model generated signals in different noisy conditions

PQ disturbances	*Sensitivity (%)(no noise)*	*Sensitivity (%)(30db noise)*	*Sensitivity (%)(35db noise)*	*Sensitivity (%)(40db noise)*
D1	98.83	98.12	98.35	98.57
D2	99	98	98.51	98.71
D3	98.14	97.43	97.64	97.86
D4	98.23	97.67	97.82	98.1
D5	99.27	98.37	98.59	98.89
D6	97.92	97.15	97.49	97.72
D7	97.13	96.43	96.71	96.87
D8	96.72	96.08	96.25	96.43
Average	98.15	97.41	97.67	97.89

Table 10 Classification accuracy (%) of the proposed method using model signals with different classifiers

PQ disturbances	*DT (%)*	*Fuzzy DT (%)*	*Improved fuzzy DT (%)*
D1	97.80	98	98.83
D2	97.95	98.23	99
D3	97.87	98.15	98.14
D4	97.23	97.53	98.23
D5	98.25	98.61	99.27
D6	97	97.12	97.91
D7	97	97	97.12
D8	96.1	96.25	96.71
Average	97.4	97.61	98.15

Figure 9 Classification accuracy of model generated different PQ events with different classifiers (see online version for colours)

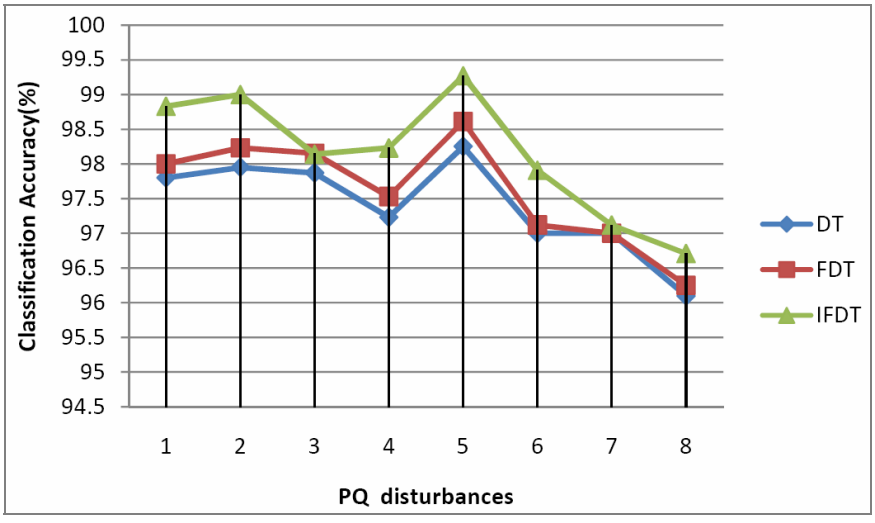

Table 11 Performance comparison of the proposed method with other existing methods

Different types of classifier	*Accuracy (%)*
WT and inductive inference approach (Abdel-Galil et al., 2004)	90.4
S-transform with modular NN (Bhende et al., 2008)	95.5
Neural network (Kezunovic and Rikalo, 1996)	95.93
WT with neural fuzzy (Huang et al., 2002)	96.5
WPD with SVM (Tong et al., 2006)	97.25
S-transform with PNN (Mishra et al., 2008)	97.4
HHT with balanced neural tree (Biswal et al., 2014)	97.9
WT with fuzzy SVM (Hu et al., 2005)	98
Proposed method (HHT with IFDT)	98.15

All the certainty factor values for different rules have been given in Table 6. Table 7 represents the confusion matrix of the microgrid model generated disturbance signals. The confusion matrix represents the overall performance of the data set of PQ disturbances, where the diagonal matrix shows the correctly classified PQ disturbances and the off diagonal matrix shows the misclassification of PQ disturbances. The performance of the proposed method in noisy and noisy free conditions was checked through the accuracy and sensitivity of the PQ disturbance classification and all the results are given in Table 8 and Table 9. Classification accuracy of different noisy conditions is clear from Figure 8, where we can see the proposed method is also acceptable in noisy condition. The classification accuracy of the improved fuzzy rules have been checked with the other classifiers such as decision tree (DT) and the FDT and it has been found that IFDT produce much better results which is clear from Figure 9. All the classification values with different classification techniques are given in Table 10.

The performance comparison of the proposed method with other established methods have been done and all the results are given in Table 11.

7 Conclusions

This paper proposes a combined technique of discrete HHT with IFDT-based detection and classification of PQ disturbances in a microgrid scenario as a new contribution to the literature. Further depending upon the overlapping values of the target feature sets a certainty factor-based IFDT has been incorporated for classifying the PQ disturbances. The proposed method has been tested for both the synthetic as well as microgrid model generated signals. The classification accuracy of the proposed method is very much significant as compared to some other conventional established techniques. The proposed method has been found very effective in different noisy conditions also.

References

Abdel-Galil, T.K., Kamel, M., Youssef, A.M., El-Saadany, E.F. and Salama, M.M.A. (2004) 'Power quality disturbance classification using the inductive inference approach', *IEEE Transactions on Power Delivery*, Vol. 19, No. 4, pp.1812–1818.

Abdullah, A.R., Sha'ameri, A.Z. and Saad, N.M. (2007) 'Power quality analysis using spectrogram and gabor transformation', In *Asia-Pacific Conference on Applied Electromagnetics*, APACE 2007, IEEE, pp.1–5.

Bhende, C.N., Mishra, S. and Panigrahi, B.K. (2008) 'Detection and classification of power quality disturbances using S-transform and modular neural network', *Electric Power Systems Research*, Vol. 78, No. 1, pp.122–128.

Biswal, B., Biswal, M., Mishra, S. and Jalaja, R. (2014) 'Automatic classification of power quality events using balanced neural tree', *IEEE Transactions on Industrial Electronics*, Vol. 61, No. 1, pp.521–530.

Biswal, M. and Dash, P.K. (2013) 'Measurement and classification of simultaneous power signal patterns with an Stransform variant and fuzzy decision tree', *IEEE Transactions on Industrial Informatics*, Vol. 9, No. 4, pp.1819–1827.

Chandel, A.K., Guleria, G. and Chandel, R. (2008) 'Classification of power quality problems using wavelet-based artificial neural network', In *Transmission and Distribution Conference and Exposition*, T&D, IEEE/PES, IEEE, pp.1–5.

Chang, N-F., Chen, T-C., Chiang, C-Y. and Chen, L-G. (2011) 'Online empirical mode decomposition biomedical microprocessor for Hilbert Huang transform', in *2011 IEEE Biomedical Circuits and Systems Conference (BioCAS)*, IEEE, pp.420–423.

Chen, S. and Zhu, H.Z. (2007) 'Wavelet transform for processing power quality disturbances', *EURASIP Journal on Applied Signal Processing*, No. 1, pp.176–176, https://doi.org/10.1155/2007/47695.

Dash, P.K., Panigrahi, B.K. and Panda, G. (2003) 'Power quality analysis using S-transform', *IEEE Transactions on Power Delivery*, Vol. 18, No. 2, pp.406–411.

Eristi, H., Yıldırım, Ö., Eristi, B. and Demir, Y. (2014) 'Automatic recognition system of underlying causes of power quality disturbances based on S-transform and extreme learning machine', *International Journal of Electrical Power and Energy Systems*, October, Vol. 61, pp553–562, https://doi.org/10.1016/j.ijepes.2014.04.010.

Espinosa, A.G., Rosero, J.A., Cusido, J., Romeral, L. and Ortega, J.A. (2010) 'Fault detection by means of Hilbert Huang transform of the stator current in a PMSM with demagnetization', *IEEE Transactions on Energy Conversion*, Vol. 25, No. 2, pp.312–318.

Gu, Y.H. and Bollen, M.H.J. (2000) 'Time-frequency and time-scale domain analysis of voltage disturbances', *IEEE Transactions on Power Delivery*, Vol. 15, No. 4, pp.1279–1284.

Hu, G-S., Xie, J. and Zhu , F-F. (2005) 'Classification of power quality disturbances using wavelet and fuzzy support vector machines', in *Proceedings of 2005 International Conference on Machine Learning and Cybernetics*, IEEE, Vol. 7, pp.3981–3984.

Huang, J., Negnevitsky, M. and Nguyen, D.T. (2002) 'A neural-fuzzy classifier for recognition of power quality disturbances', *IEEE Transactions on Power Delivery*, Vol. 17, No. 2, pp.609–616.

Janik, P. and Lobos, T. (2006) 'Automated classification of power-quality disturbances using SVM and RBF networks', *IEEE Transactions on Power Delivery*, Vol. 21, No. 3, pp.1663–1669.

Jurado, F. and Saenz, J.R. (2002) 'Comparison between discrete STFT and wavelets for the analysis of power quality events', *Electric Power Systems Research*, Vol. 62, No. 3, pp.183–190.

Kaewarsa, S. (2009) 'Classification of power quality disturbances using S-transform-based artificial neural networks', *IEEE International Conference on Intelligent Computing and Intelligent Systems*, ICIS 2009, IEEE, Vol. 1, pp.566–570.

Kaewarsa, S. (2009) 'Classification of power quality disturbances using S-transform-based artificial neural networks', in *IEEE International Conference on Intelligent Computing and Intelligent Systems*, ICIS 2009, IEEE, Vol. 1, pp.566–570.

Kezunovic, M. and Rikalo, I. (1996) 'Detect and classify faults using neural nets', *IEEE Computer Applications in Power*, Vol. 9, No. 4, pp.42–47.

Lee, I.W.C. and Dash, P.K. (2003) 'S-transform-based intelligent system for classification of power quality disturbance signals', *IEEE Transactions on Industrial Electronics*, Vol. 50, No. 4, pp.800–805.

Lee, J., Tiao, A. and Yen , J. (1994) 'A fuzzy rule-based approach to real-time scheduling', in *IEEE World Congress on Computational Intelligence, Proceedings of the Third IEEE Conference on Fuzzy Systems*, IEEE, pp.1394–1399.

Li, X., Tso, S.K. and Wang, J. (2000) 'Real-time tool condition monitoring using wavelet transforms and fuzzy techniques', *IEEE Transactions on Systems, Man, and Cybernetics, Part C (Applications and Reviews)*, Vol. 30, No. 3, pp.352–357.

Mishra, S., Bhende, C.N. and Panigrahi, B.K. (2008) 'Detection and classification of power quality disturbances using Stransform and probabilistic neural network', *IEEE Transactions on Power Delivery*, Vol. 23, No. 1, pp.280–287.

Pei, S.C. and Yeh, M.H. (2000) 'Discrete fractional Hilbert transform', *IEEE Trans. Circuits Syst. II*, November, Vol. 47, No. 11, pp.1307–1311.

Santoso, S., Grady, W.M., Powers, E.J., Lamoree, J. and Bhatt, S.C. (2000) 'Characterization of distribution power quality events with Fourier and wavelet transforms', *IEEE Transactions on Power Delivery*, Vol. 15, No. 1, pp.247–254.

Tong, W., Song, X., Lin, J. and Zhao, Z. (2006) 'Detection and classification of power quality disturbances based on wavelet packet decomposition and support vector machines', in *2006 8th International Conference on Signal Processing*, IEEE, Vol. 4.